INFLUENCE OF THE REFLECTION OF RADIATION ON RADIATIVE – CONVECTIVE HEAT EXCHANGE DURING HYPERSONIC FLOW OVER BLUNT BODIES

M. N. Rolin, R. I. Soloukhin,
and F. B. Yurevich

UDC 533.6.011.55:536.244

The influence of the reflection of radiant energy from the surface on the flow and heat-exchange characteristics has not been considered in reports on the investigation of radiative–convective heat exchange during hypersonic flow over blunt bodies and of flows of a radiating gas beyond a compression shock [1-5]. It is interesting to make calculations of radiative–convective heat exchange with allowance for the reflection of radiation from the surface of the body in order to determine the influence of this effect on the values of the radiant and convective fluxes to the wall. Since a physical effect is being estimated, as an example it is desirable to be confined to the consideration of the conditions in the vicinity of the stagnation point of an axisymmetric blunt body over which a hypersonic air stream flows. In this case one can expect that the absorption of radiation reflected from the wall will lead to the redistribution both of the temperature field in the boundary layer and of the balance of radiative losses of the emitting layer.

We use a system of equations describing the flow of a viscous, heat-conducting, equilibrium-reacting, radiating gas in the vicinity of the axis of symmetry of the stream. This system of equations is obtained as an asymptotic approximation of the general Navier–Stokes equations for high Mach and Reynolds numbers [6]. In the coordinate system shown in Fig. 1 it has the following form:

$$2\rho\left(\frac{\partial u}{\partial x}\right)+\frac{\partial}{\partial y}(\rho v)=0; \tag{1}$$

$$\rho\left(\frac{\partial u}{\partial x}\right)^2+\rho v\frac{\partial}{\partial y}\left(\frac{\partial u}{\partial x}\right)=-\frac{\partial^2 p}{\partial x^2}+\frac{\partial}{\partial y}\left[\mu\frac{\partial}{\partial y}\left(\frac{\partial u}{\partial x}\right)\right]; \tag{2}$$

$$\frac{\partial p}{\partial y}=0; \tag{3}$$

$$\rho v\frac{\partial H}{\partial y}=-\frac{\partial}{\partial y}\left(-\lambda\frac{\partial T}{\partial y}+\sum_j H_jJ_j+q^{\mathrm{r}}\right); \tag{4}$$

$$\rho v\frac{\partial c_k^*}{\partial y}=-\frac{\partial}{\partial y}J_k^*, \tag{5}$$

where

$$c_k^*=\sum_j\gamma_{kj}c_j;\qquad J_k^*=\sum_j\gamma_{kj}J_j;$$

u and v are the velocity components; ρ is the gas density; p is the pressure; H is the enthalpy per unit mass; q^r is the radiative flux; μ is the viscosity; λ is the thermal conductivity; H_j is the specific enthalpy of a chemical component; J_j is the diffusional mass flux of a component; c_j is the mass concentration of a component; J_k^* is the diffusional mass flux of a chemical element; c_k^* is the mass concentration of a chemical element; γ_{kj} is the mass content of chemical element k in component j. The conditions in the undisturbed stream, directly behind the compression shock, and at the wall will be denoted by the subscripts ∞, s, and w, respectively.

The possibility of using the condition of constancy of the pressure across the compressed layer (3) was confirmed by calculations [4]. The system of equations (1)-(5) is closed by the condition

$$\frac{\partial^2 p}{\partial x^2}=-\frac{8}{3}\rho_\infty\frac{v_\infty^2}{R^2}$$

Minsk. Translated from Zhurnal Prikladnoi Mekhaniki i Tekhnicheskoi Fiziki, No. 2, pp. 99-107, March-April, 1980. Original article submitted April 24, 1979.

0021-8944/80/2102-0239$07.50 © 1980 Plenum Publishing Corporation

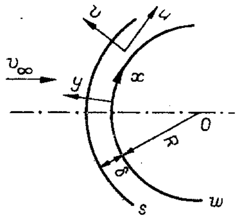

Fig. 1

for the longitudinal pressure gradient [4]. The generalized Rankine–Hugoniot equations are used as the boundary conditions [6]:

$$\rho_\infty v_\infty = -(\rho v)_s, \quad \rho_\infty v_\infty^2\left(1-\frac{\rho_\infty}{\rho_s}\right)+p_\infty = p_s,$$
$$\rho_\infty v_\infty\left[\frac{v_\infty}{R}-\left(\frac{\partial u}{\partial x}\right)_s\right]=\left[\mu\frac{\partial}{\partial y}\left(\frac{\partial u}{\partial x}\right)\right]_s,$$
$$\rho_\infty v_\infty\left[H_\infty+\frac{v_\infty^2}{2}-H_s\right]=-\left[-\lambda\frac{\partial T}{\partial y}+\sum_j H_j J_j\right]_s,$$
$$\rho_\infty v_\infty\left[c_{k\infty}^*-c_{ks}^*\right]=-J_{ks}^*. \tag{6}$$

The influence of advance radiation was ignored. The conditions

$$v_w=0, \quad u_w=0, \quad T=T_w, \quad J_{kw}^*=0 \tag{7}$$

were assigned at the wall. The diffusional fluxes and the coefficients of viscosity and thermal conductivity were determined by the method of [7]. Effects of multicomponent diffusion and the presence of ionization in the gas mixture were allowed for. In calculating the composition it was assumed that local thermodynamic equilibrium occurs in the compressed layer.

The approximation of an infinite plane layer [1-4] was used to determine the radiant heat fluxes. The expressions for q^r can be obtained from the radiation-transfer equation,

$$q^r=\int_0^\infty q_\nu^r d\nu,$$
$$q_\nu^r(\tau)=2\pi\int_0^{\tau_s} B_\nu(\tau')E_2(|\tau-\tau'|)\,\mathrm{sgn}(\tau-\tau')\,d\tau'+\Delta q_{\nu w}(\tau), \tag{8}$$

where ν is the frequency or wave number; B_ν is the Planck function; $\tau=\int_0^y k_\nu(y')\,dy'$ is the optical depth; k_ν is the coefficient of absorption; $\Delta q_{\nu w}$ is the contribution of radiation from the wall; $E_n(\tau)$ is the symbol for an integroexponential function of order n.

The reflectivity and emissivity of the wall were assumed to be isotropic. In the cases of diffusely and specularly reflecting surfaces we have

$$\Delta q_{\nu w}^d=2\pi(1-r_\nu)B_{\nu w}E_{sp}(\tau)+2\pi r_\nu E_3(\tau)\int_0^{\tau_s}B_\nu(\tau')E_2(\tau')\,d\tau'; \tag{9}$$

$$\Delta q_{\nu w}^{sp}=2\pi(1-r_\nu)B_{\nu w}E_{sp}(\tau)+2\pi r_\nu\int_0^{\tau_s}B_\nu(\tau')E_2(\tau+\tau')\,d\tau', \tag{10}$$

respectively, where r_ν is the coefficient of reflection.

The contributions of both the continuous emission spectrum and the spectral lines of atoms and ions were allowed for in the calculations. The entire significant range of wave numbers (10^3-$2\cdot10^5$ cm^{-1}) was divided into a series of regions, in each of which the coefficient of absorption of the continuous spectrum was assumed to be constant. The radiation transfer in spectral lines was determined using the Curtis–Hodgson method [8]. The procedure of [9] was used to allow for the multiplet structure. The first terms of spectral series, including the strongest lines, were allowed for individually. Higher terms of series were allowed for using Goody's statistical model [8, 10].

The use of the equations of the Curtis–Hodgson method and Goody's statistical model with allowance for the superposition of the continuous and line spectra was provided for through the use of the exponential approximation for the integroexponential functions appearing in (8)-(10). The essence of this procedure consists in the following:

by definition

$$E_n(\tau) = \int_1^{\infty} \frac{e^{-\tau r}}{p^n}\, dp,$$

which is identical to

$$E_n(\tau) = \int_{-1}^{1} \left(\frac{x+1}{2}\right)^{n-2} e^{-\frac{2\tau}{x+1}} dx,$$

and this integral can be found approximately using a Gaussian quadrature [11], which gives

$$E_n(\tau) \approx \sum_{k=1}^{m} w_k \left(\frac{x_k+1}{2}\right)^{n-2} e^{-\frac{2\tau}{x_k+1}},$$

where w_k and x_k are the weights and ordinates of the Gaussian quadrature, the values of which are available in [11] for different m. Numerical calculations show that one can be confined to m = 3 with sufficient accuracy for practical purposes (an error of less than 1% for one-sided radiant fluxes in the compressed layer).

In constructing a model of the optical properties of air we used data on the absorption cross sections and the parameters of spectral lines taken from [12]. The spectrum was divided into 32 intervals with constant coefficients of continuous absorption. Individual allowance was made for 109 spectral multiplets of nitrogen and oxygen atoms and ions. In addition, the model included six systems of higher terms of spectral series adjacent to the photoionization thresholds of the ground-level electron configurations of the atoms. A comparison of the results of calculations of the emissivities of isothermal volumes of air with the data of [12] showed that in all the significant intervals the difference does not exceed 10-15%. A numerical method of solving the system of equations (1)-(5) with the boundary conditions (6) and (7) is described in [13].

Since we are talking about an estimate of the maximum possible effect of the influence of the reflection of radiant energy from the wall on radiative–convective heat exchange, we can be confined to the case of a coefficient of reflection r_ν not dependent on the wave number. Here we must consider that significant absorption of the reflected radiation takes place in the short-wavelength part of the spectrum, i.e., in the vacuum ultraviolet region ($\nu > 60{,}000$ cm^{-1}). Short-wavelength radiation reflected from the wall, being absorbed in the relatively cool boundary region of the compressed layer, should cause an increase in the temperature gradient and hence in the convective heat flux to the wall. The effect of radiative cooling should be reduced as a result of the absorption of reflected radiation in the high-temperature region of the compressed layer, which leads to an increase in the radiant flux in the entire spectral range. One more effect is connected with the above-noted increase in the temperature gradient in the boundary region, which is equivalent to a decrease in its thickness and hence to a decrease in the ability to shield the wall from radiation in the vacuum ultraviolet region.

These arguments are supported by the results of the numerical calculations, which were carried out for the following conditions: velocity of oncoming stream $1.4 \cdot 10^4$ m/sec $\leq v_\infty \leq 1.8 \cdot 10^4$ m/sec; stagnation pressure 0.3 atm $< p_s <$ 30 atm; blunting radius 0.3 m $< R <$ 3 m. In all cases below where it is not specifically stated, the surface temperature was taken as 2500°K, while the reflection was assumed to be diffuse.

First of all, it was discovered that the rise in the convective and the one-sided radiant fluxes q_w^c and q_w^{r-} to the wall is roughly proportional to the value of the coefficient of reflection r, in connection with which it proved expedient to characterize these effects by the quantities

$$a^r = \frac{q_{w1}^{r-} - q_{w0}^{r-}}{q_{w0}^{r-}}; \tag{11}$$

$$a^c = \frac{q_{w1}^{c} - q_{w0}^{c}}{q_{w0}^{c}}, \tag{12}$$

where the subscripts 1 and 0 denote quantities obtained with r = 1 and r = 0, respectively.

Since calculations of a radiation field with allowance for spectral lines require large expenditures of computer time, only the continuous spectrum was allowed for in a considerable share of the variants. The corresponding results are presented in Table 1. It is seen that the effect of the influence of reflection on the values of the radiant and convective fluxes to the wall, expressed by the quantities a^r and a^c of (11) and (12), grows with an increase in velocity, stagnation pressure, and blunting radius. Here the influence of the velocity is due

TABLE 1

$v_\infty \cdot 10^{-4}$, m/sec	p_s, atm	R, m	$q^{r-}_{wo} \cdot 10^{-7}$, W/m²	$q^{c}_{wo} \cdot 10^{-7}$, W/m²	a^r	a^c
1,8	0,3	0,3	0,58	2,03	0,000	**0,059**
		1,0	1,13	1,31	0,035	**0,176**
		3,0	1,72	0,90	0,064	**0,288**
	1,0	0,3	3,22	4,36	0,031	0,158
		1,0	5,02	2,80	0,066	0,286
		3,0	7,28	1,53	0,068	0,386
	3,0	0,3	12,5	8,64	0,056	0,239
		1,0	18,8	4,49	0,074	0,385
1,6	0,3	1,0	0,87	1,06	0,032	0,151
	1,0		3,93	2,16	0,056	0,240
	3,0		15,5	3,46	0,058	0,313
	10,0	0,3	39,9	11,3	0,060	0,293
		1,0	65,2	5,38	0,076	0,424
1,4	0,3	1,0	0,56	0,82	0,025	0,117
	1,0		2,66	1,59	0,037	0,181
	3,0		11,0	2,58	0,045	0,228
	10,0		49,1	4,29	0,063	0,300
	30,0	0,3	101,0	13,8	0,049	0,283

to an increase in the temperature in the compressed layer and hence an increase in the radiant flux in the vacuum ultraviolet region arriving at the wall, while the influence of the radius and the pressure is due to an increase in the absorption of reflected radiation.

The calculations with allowance for radiation transfer in spectral lines were made in the range of stagnation pressures of 0.3–3 atm. The results of these calculations are presented in Table 2. The values of the radiant fluxes to the wall prove to be higher in this case, while the values of the convective fluxes are lower than the values obtained with allowance for the continuous spectrum only. The latter fact is explained by the intensification of radiative cooling of the compressed layer, which leads to a decrease in its temperature. The values of the quantities a^r and a^c prove to be larger, which is due to strong self-absorption in the line spectrum. In this case, however, the qualitative character of the dependence of these quantities on the velocity, stagnation pressure, and blunting radius remains as before. Data on the spectral distribution of the radiative heat flux to the surface are presented in Figs. 2 and 3. In Fig. 2 we give the dependences on ν for the relative value of the monochromatic radiative flux, while in Fig. 3 we give the values of the quantity

$$b_\nu = \frac{\int_0^\nu q^{r-}_{\nu w} d\nu}{q^{r-}_w},$$

convenient for determining the contributions of separate regions of the spectrum. Line 1 corresponds to the case of v_∞ = 18 km/sec, R = 1 m, and p_s = 1 atm with allowance for spectral lines; line 2 corresponds to the

TABLE 2

$v_\infty \cdot 10^{-4}$, m/sec	p_s, atm	R, m	$q^{r-}_{wo} \cdot 10^{-7}$, W/m²	$q^{c}_{wo} \cdot 10^{-7}$, W/m²	a^r	a^c
1,8	0,3	1,0	1,63	1,20	0,055	0,208
		3,0	2,25	0,76	0,080	0,330
	1,0	1,0	6,71	2,37	0,082	0,339
		3,0	8,93	1,22	0,103	0,476
	3,0	0,3	16,5	7,41	0,097	0,301
		1,0	23,1	3,66	0,113	0,498
1,6	0,3	1,0	1,29	0,974	0,054	0,195
	1,0		5,42	1,85	0,083	0,303
	3,0		19,3	2,92	0,103	0,424
1,4	0,3	1,0	0,871	0,767	0,050	0,145
	1,0		3,80	1,42	0,072	0,232
	3,0		14,1	2,29	0,085	0,332

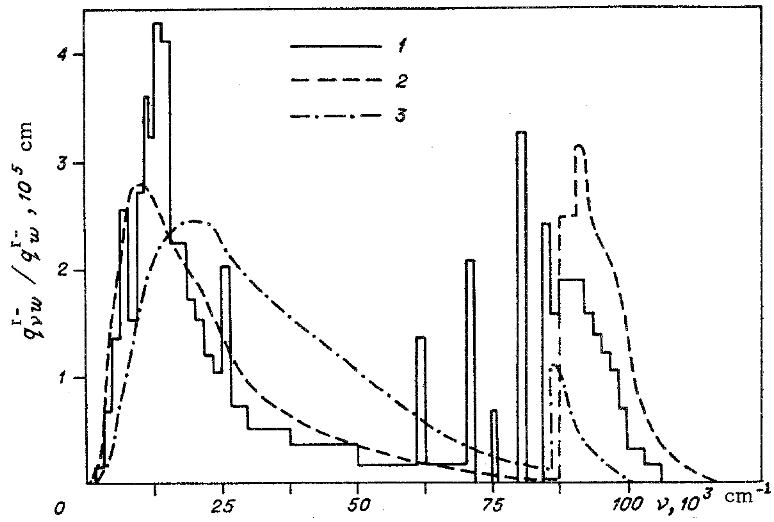

Fig. 2

same conditions with allowance for the continuous spectrum only; line 3 corresponds to v_∞ = 14 km/sec, R = 0.3 m, and p_s = 30 atm and allowance for the continuous spectrum only. Curves 2 and 3 in Fig. 2 and all the curves in Fig. 3 are smoothed. The power-law character of the dependence 1 in Fig. 2 is due to the absence of spectral resolution in the separate spectral intervals.

The following dependence for the withdrawal distance δ of the compression shock was found in [3] on the basis of numerical calculations:

$$\delta = \delta_0\left[1 - \frac{2\left(q_s^r - q_w^r\right)}{\rho_\infty v_\infty^3}\right], \tag{13}$$

where δ_0 is the withdrawal distance of the shock in the absence of radiative cooling of the compressed layer. It turned out that the dependence (13) is also valid in the case of the allowance for reflection from the wall. In this case the quantities q_s^r and q_w^r depend on r in such a way that for the conditions under consideration the value of δ for a fully reflecting wall does not exceed its value for the case of an absolutely black wall by more than 2-3%.

The character of the influence of reflection on the enthalpy distribution in a compressed layer is shown in Fig. 4, where we present data obtained with v_∞ = 18 km/sec and R = 1 m. The solid curves pertain to the case of r = 0 and the dashed curves to r = 1. Curves 1 and 2 correspond to p_s = 1 atm and curve 3 to p_s = 3 atm. Only the continuous spectrum was considered in the calculation on the basis of which curve 1 was constructed, while the results of calculations with allowance for spectral lines were used for 2 and 3. It is seen that the influence of reflection on the profile of the enthalpy distribution extends only to the boundary region.

Estimates of the influence of the surface temperature on the effect of an increase in heat fluxes are interesting. The results of calculations for two modes with values of T_w different from 2500°K are presented in Table 3. These data allow one to assume that a^r and a^c depend weakly on the surface temperature. We also calculated the radiative–convective heat exchange for a specularly reflecting surface. The values of a^r and a^c in this case differ by no more than a few percent from those obtained under the assumption of reflection of a diffuse nature.

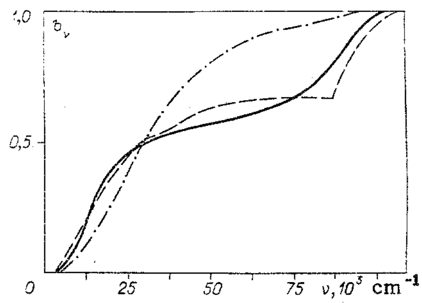

Fig. 3

TABLE 3

$v_\infty \cdot 10^{-4}$, m/sec	p_s, atm	R, m	T_w, °K	$q^{r-}_{wo} \cdot 10^{-7}$, W/m^2	$q^{c}_{wo} \cdot 10^{-7}$, W/m^2	a^r	a^c
1,8	1,0	1,0	1500	4,98	2,88	0,060	0,270
			3500	5,15	2,66	0,066	0,305
1,6	10,0	1,0	1500	64,8	5,68	0,077	0,420
			3500	65,6	4,89	0,076	0,448

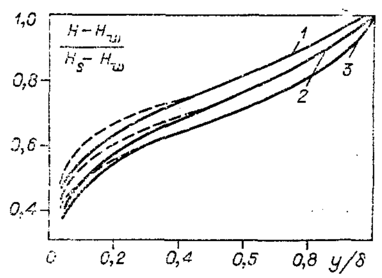

Fig. 4

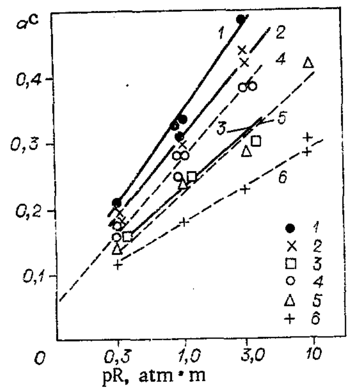

Fig. 5

The influence of the thermal self-emission of the surface was estimated with the help of a series of control calculations in which the term $\Delta q_{\nu w}$ in Eq. (8) was taken as equal to zero. A comparison of the corresponding results with data obtained for r = 0 showed that even at T_w = 3500°K the influence of the self-emission of the wall on the quantities q_w^{r-} and q_w^c did not exceed the calculation error itself. This is explained by the weak absorption by the gas of the wall thermal emission lying in the visible and infrared regions of the spectrum at low stagnation pressures and by the smallness of the ratio $2\sigma T_w^4/\rho_\infty v_\infty^3$ characterizing the radiative–convective interaction at high stagnation pressures, when absorption is important.

In analyzing the data presented in Tables 1 and 2, one can note that at fixed values of v_∞ and close values of the product of the stagnation pressure and the blunting radius (p_sR) one obtains close values of the coefficient a^c. The data of Tables 1 and 2 on the coefficients a^c are plotted in Fig. 5 on a logarithmic scale in the form of the dependence on the product (p_sR). The designations 1-3 correspond to calculations with allowance for spectral lines; 4-6 correspond to calculations without allowance for spectral lines; 1, 4) v_∞ = 18 km/sec; 2, 5) v_∞ = 16 km/sec; 3, 6) v_∞ = 14 km/sec. An approximation of the calculated points by a dependence of the type

$$a^c = K_1 \lg(p_sR) + K_2,$$

where K_1 and K_2 are constants, gave a maximum deviation not exceeding 9%. The corresponding straight lines are also presented in the graph. Thus, in the range of values of 0.3 atm • m ≤ (p_sR) ≤ 10 atm • m this quantity can serve as a parameter of approximate similarity in an analysis of the effect of intensification of the convective heat flux to a surface over which a hypersonic air stream flows as a result of the reflection of radiation.

In conclusion, we note that in the range of conditions under consideration the convective heat flux to a fully reflecting wall can exceed the flux to an absolutely black one by about 50%. The influence of the reflection of radiation on the amount of radiative flux to the wall is also important, especially at increased pressures. Judging from data on the coefficients of reflection of actual surfaces [14, 15], one can expect that allowance for these effects can lead to an increase of 10-20% in the calculated values of the heat flux into the body.

LITERATURE CITED

1. N. A. Anfimov and V. P. Shari, "Solution of the system of equations of motion of a selectively emitting gas in a shock layer," Izv. Akad. Nauk SSSR, Mekh. Zhidk. Gaza, No. 3 (1968).
2. H. Hoshizaki and K. H. Wilson, "Convective and radiative heat transfer during superorbital entry," AIAA J., 5, No. 1 (1967).

3. L. M. Biberman, S. Ya. Bronin, and A. N. Lagar'kov, "Radiative–convective heat exchange during hypersonic flow over a blunt body," Izv. Akad. Nauk SSSR, Mekh. Zhidk. Gaza, No. 5 (1972).
4. A. N. Rumynskii and V. P. Churkin, "Flow of a hypersonic stream of viscous radiating gas over a blunt body," Zh. Vychisl. Mat. Mat. Fiz., 14, No. 6 (1974).
5. V. P. Zamuraev, I. I. Maslennikova, and R. I. Soloukhin, "An investigation of radiative heat exchange behind shockwaves in air using the multigroup averaging method," in: Heat and Mass Transfer during Intense Radiant and Convective Heating [in Russian], Inst. Teplo-Massoobmena Akad. Nauk BSSR, Minsk (1977).
6. K. M. Magomedov, "Hypersonic flow of a viscous gas over blunt bodies," Izv. Akad. Nauk SSSR, Mekh. Zhidk. Gaza, No. 2 (1970).
7. M. N. Rolin, F. B. Yurevich, and V. V. Kondrashov, "An approximate method of calculating transfer coefficients for partially ionized gas mixtures," Inzh.-Fiz. Zh., 24, No. 3 (1978).
8. K. S. Adzerikho, Lectures on the Theory of Radiant Energy Transfer [in Russian], Belorus. Gos. Univ. im. V. I. Lenina, Minsk (1975).
9. M. N. Rolin, "The approximate calculation of radiation transfer in spectral multiplets," in: Some Problems of Heat and Mass Exchange [in Russian], Inst. Teplo-Massoobmena Akad. Nauk BSSR, Minsk (1978).
10. R. M. Goody, Atmospheric Radiation, Clarendon Press, Oxford (1964).
11. V. I. Krylov, The Approximate Calculation of Integrals [in Russian], Nauka, Moscow (1967).
12. I. V. Avilova, L. M. Biberman, et al., Optical Properties of Hot Air [in Russian], Nauka, Moscow (1970).
13. M. N. Rolin and F. B. Yurevich, "An economical means of calculating flows in the vicinity of a stagnation point," in: Heat and Mass Transfer during Intense Radiant and Convective Heating [in Russian], Inst. Teplo-Massoobmena Akad. Nauk BSSR, Minsk (1977).
14. A. N. Zaidel' and E. Ya. Shreider, Spectroscopy of the Vacuum Ultraviolet [in Russian], Nauka, Moscow (1972).
15. I. K. Kikoina (editor), Tables of Physical Quantities. Handbook [in Russian], Atomizdat, Moscow (1976).

EXPERIMENTAL INVESTIGATION OF LOW-DENSITY PULSED SUPERSONIC JETS

V. A. Kochnev and I. M. Naboko

UDC 534.222.2

1. The present report is a continuation of [1, 2], in which we presented the results of an experimental investigation, by the method of electron-beam probing, of pulsed jets of Ar and N_2 formed by discharge from a sonic nozzle with a diameter $d_* = 0.25$ mm at an initial pressure $p_0 = 7$–8 atm, an ambient pressure $p_\infty = (1.5\text{–}2) \cdot 10^{-5}$ mm Hg, and temperatures $T_0 = T_\infty = 300$°K.

A description of the experimental complex and the procedure is given in [1]. In the present work we experimentally investigated pulsed Ar and N_2 jets discharging through a conical supersonic nozzle into a space with a counterpressure $p_\infty = 2 \cdot 10^{-5}$ mm Hg. The gas pressure p_0 in the reservoir was 2 atm and the expansion ratio was $N = p_0/p_\infty = 10^8$. The radii of the critical and exit cross sections of the nozzle were $r_* = 0.835$ and $r_a = 4$ mm, respectively, and the expansion angle was $\alpha = 43°$. The calculated Mach numbers were $M_a = 4.9$ for N_2 and 6.9 for Ar. An electromagnetic valve employed at the FIRÉ, Academy of Sciences of the USSR, was mounted at the nozzle entrance. The valve was opened by a powerful current pulse supplied to the solenoid of the valve. Then the plunger located inside the solenoid and covering the nozzle entrance was shifted and the gas entered the nozzle.

The signals of electron-beam absorption were recorded at distances $X = x/r_a = 50$–320 along the axis and up to $Y = y/r_a = 150$ from the axis of the stream in both directions.

Four stages of the process are recorded on oscillograms of beam-current absorption: the appearance and steep rise of the absorption signal, a region of sharp variation of the derivative of variation of the signal with a subsequent slow rise in the process of development of the flow, a relatively constant level of absorption,

Moscow. Translated from Zhurnal Prikladnoi Mekhaniki i Tekhnicheskoi Fiziki, No. 2, pp. 107–113, March–April, 1980. Original article submitted April 5, 1979.

0021-8944/80/2102-0245$07.50 © 1980 Plenum Publishing Corporation